

Spin transfer torque switching in pentalayer nanopillar with biquadratic coupling

D. Aravinthan,¹ P. Sabareesan,² and M. Daniel^{1,3, a)}

¹⁾ Centre for Nonlinear Dynamics, School of Physics, Bharathidasan University, Tiruchirappalli - 620 024, Tamilnadu, India

²⁾ Centre for Nonlinear Science and Engineering, School of Electrical and Electronics Engineering, SASTRA University, Thanjavur - 613 401, Tamilnadu, India

³⁾ SNS Institutions, Coimbatore - 641 049, Tamilnadu, India

The effect of biquadratic coupling on spin transfer torque assisted magnetization switching in the pentalayer nanopillar device is studied by numerically solving the magnetization switching dynamics of the free layer governed by the Landau-Lifshitz-Gilbert-Slonczewski (LLGS) equation. Magnetization switching time in the absence of biquadratic coupling for an applied current density of $10 \times 10^{11} \text{Am}^{-2}$ is 186 ps. Biquadratic coupling arises due to the uncorrelated roughness in the ferromagnetic layers and it reduces the switching time to 160 ps. Further, the impact of the period of the roughness and spacer layer thickness on switching time is studied.

Keywords: Ultrafast magnetization dynamics, magnetization switching, spin transfer torque, nanopillar, switching time.

I. INTRODUCTION

Ultrafast magnetization switching assisted by a spin transfer torque has been received considerable interest in recent years, due to its potential applications in future spintronic devices such as magnetic random access memories^{1,2} and high frequency microwave oscillators^{3,4}. The basic structure used in the memory devices is a trilayer structure consists of two ferromagnetic layers and a nonmagnetic spacer layer. In which, magnetization of the first ferromagnetic layer is fixed and hence it act as a polarizer, when the current passes through it. Spin polarized electrons reaches the second ferromagnetic layer (free layer), produces a spin torque due to the exchange interaction between local magnetization and spin angular momentum⁵. This spin torque will switch the magnetization of the free layer, when the applied current is above the critical value⁶. The reduction of the critical current density and the switching time are the two important issues in the development of potential applications. Fuchs et al⁷ introduced a pentalayer structure based on the proposal from Berger⁸, in order to reduce the critical current density and the switching time by increasing the spin transfer torque efficiency. In the pentalayer structure, additional spacer layer and a ferromagnetic pinned layer are added above the trilayer structure and showed that spin torque efficiency is increased, when the pinned layers are anti-aligned⁹. The enhanced spin transfer torque increases the switching speed and reduces the switching time and critical current density required to initiate the magnetization switching^{10,11}. Since, then spin transfer torque magnetization switching in pentalayer nanopillar has been widely studied both theoretically¹²⁻¹⁵ and experimentally^{16,17}. Growing a pentalayer nanopillar for

magnetization switching applications in a smooth fashion without roughness is very difficult. Hence, the resultant pentalayer structure have certain interface roughness, and they give rise to two different coupling mechanisms¹⁸. First one is biquadratic coupling which arises due to the uncorrelated interface roughness¹⁹ and the second one is orange peel coupling (Néel coupling) which arises due to the correlated interface roughness²⁰. We have recently studied the effect of both orange peel coupling²¹ and biquadratic coupling²² on current induced magnetization switching in trilayer structure. In this paper, we study the effect of biquadratic coupling on spin torque magnetization switching in a pentalayer nanopillar device. Biquadratic coupling was first phenomenologically introduced by Rühlig et al in 1991²³. The energy expression describing two coupled magnetic layers of the form $\frac{E}{A} = -J_2(\mathbf{m}_1 \cdot \mathbf{m}_2)^2$, is called as biquadratic, because it is quadratic in both of the magnetization directions¹⁸. Where, E and A are the energy and unit surface area of the interface respectively. \mathbf{m}_1 and \mathbf{m}_2 are unit magnetization vectors of the first and second magnetic layers respectively. J_2 is the coupling strength. All the measured values of J_2 is negative, favoring perpendicular orientations of the magnetizations. Biquadratic coupling can be experimentally studied by measuring the field dependence of the direction and value of the macroscopic magnetic moment of the sample. There are various technique which provide this information, such as Magneto-optical Kerr effect (MOKE), magnetometry, vibrating sample magnetometry (VSM), superconducting quantum interface device (SQUID) magnetometry, alternating gradient magnetometry (AGM), etc²⁴. The first hints for the existence of the biquadratic in Fe/Cr/Fe trilayer were observed independently by Grünberg et al²⁵ and Unguris et al²⁶ in 1991. Existence of biquadratic was firmly established by Rühlig et al²³ and it has been investigated in detail by many people²⁷⁻³⁴. Although biquadratic was studied for many systems, there is no

^{a)} Electronic mail: danielcnld@gmail.com

general theory for biquadratic coupling which can be adopted for all the systems. Biquadratic coupling arises due to anyone of the following origin: intrinsic origin (angular dependence of exchange energy)^{35–39}, extrinsic thickness fluctuations^{40,41}, indirect exchange through unpaired spin (“loose spin” model)⁴², and uncorrelated roughness interface^{19,43}. We investigate the effect of biquadratic coupling occurs due to the magnetic dipole field created by a uncorrelated roughness in the ferromagnetic layers. This can be done by solving the magnetization switching dynamics of the free layer governed by the Landau-Lifshitz-Gilbert-Slonczewski (LLGS) equation. The structure of the paper is organized as follows. Sketch of the pentaplayer nanopillar taken for our study and the construction of the dynamical equation (LLGS) expressing the magnetization switching dynamics of the free layer are described in section II. Numerical integration of the LLGS equation and the results are discussed in section III. Concluding remarks are made in section IV.

II. MODEL WITH BIQUADRATIC COUPLING AND DYNAMICAL EQUATION

The pentaplayer nanopillar structure consists of three ferromagnetic layers (two pinned layer and one free layer) and two non-magnetic metal (spacer) layers are taken for our study and the schematic diagram of the pentaplayer nanopillar are given in FIGURE 1. Magnetization of the first pinned layer (bottom) having large thickness is pinned along the easy axis. Thickness of the second

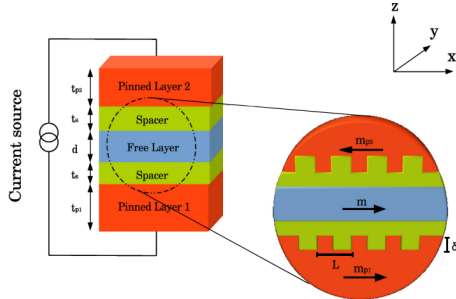


FIG. 1. A sketch of the pentaplayer nanopillar with biquadratic coupling. In the zoomed view, we see the pinned layers have the periodic interfacial terraces with a period L and a height δ . \mathbf{m} , \mathbf{m}_{p1} and \mathbf{m}_{p2} represent the magnetization of the free layer, first pinned layer and second pinned layer respectively.

pinned layer (top) is lower than the first one and its magnetization is pinned opposite to that of first one, in order to increase the spin transfer efficiency. Both pinned layers have periodic interfacial roughness with a period L and a height δ . Thickness of the free layer is thinner than the second pinned layer, and its magnetization is

free to move and it have in-plane anisotropy. Two thinner non-magnetic metal spacers are taken in between the ferromagnetic layers to avoid the direct coupling between the ferromagnetic layers. Current is supplied normal to the plane of the device (z-direction) and it becomes spin polarized, when passes through the pinned layer. The polarized current entered into the interface of the free layer produces a spin transfer torque (STT) due to the exchange coupling between the spins of the conduction electron and local magnetization, and it switches the magnetization of the free layer. The electrons scattered from the free layer reaches the second pinned layer. Since the magnetization of the second pinned layer is anti-aligned to the free layer (high resistance configuration) and hence the electrons are reflected back into the free layer. The reflected electrons produces an additional STT in the free layer, which reduces the critical current density and the switching time. The magnetization switching dynamics of the free layer in the pentaplayer is governed by the LLGS equation and it can be written in dimensionless form as⁴⁴,

$$\frac{d\mathbf{m}}{d\tau} = -[\mathbf{m} \times \mathbf{h}_{\text{eff}}] - \alpha[\mathbf{m} \times (\mathbf{m} \times \mathbf{h}_{\text{eff}})] + a_{j1}[\mathbf{m} \times (\mathbf{m} \times \mathbf{m}_{p1})] - a_{j2}[\mathbf{m} \times (\mathbf{m} \times \mathbf{m}_{p2})]. \quad (1a)$$

$$\mathbf{m} = (m^x, m^y, m^z), \quad \mathbf{m}^2 = m^x^2 + m^y^2 + m^z^2 = 1. \quad (1b)$$

Where, $\mathbf{m} = \frac{\mathbf{M}}{M_s}$ is the dimensionless magnetization of the free layer, $\tau = \gamma M_s t$ is the dimensionless time variable. Here γ is gyromagnetic ratio, M_s is saturation magnetization of the free layer. α is the Gilbert damping parameter, $a_{j1} = \frac{pJ\hbar}{\mu_0 e d M_s M_{sp1}}$ and $a_{j2} = \frac{pJ\hbar}{\mu_0 e d M_s M_{sp2}}$ are the spin transfer torque coefficient due to the first and second pinned layer respectively. Spin transfer torque coefficient value is positive when electrons flow from the pinned layer to the free layer (i.e. thicker layer to thinner layer) and negative when the electrons transfer from the free layer to the pinned layer (i.e. thinner to thicker layer)^{6,45}. Here, p is the polarization factor, J is the current density applied, \hbar is reduced Planck's constant, μ_0 is the permeability of the free space, e is the electrons charge, d is the thickness of the free layer and M_{sp1} and M_{sp2} represents the saturation magnetization of the first pinned layer and second pinned layer respectively. \mathbf{m}_{p1} and \mathbf{m}_{p2} are the unit magnetization vectors in the first and second pinned layers respectively. To account the non-collinearity between the free layer easy axis and pinned layer magnetization, we shall write the pinned layers magnetization as $\mathbf{m}_{p1} = \cos \theta_1 \mathbf{e}^x + \sin \theta_1 \mathbf{e}^y$ and $\mathbf{m}_{p2} = \cos(\pi + \theta_2) \mathbf{e}^x + \sin(\pi + \theta_2) \mathbf{e}^y$, where, θ_1 and θ_2 are the angles between the free layer easy axis and the magnetization of the first and second pinned layers respectively. The effective magnetic field \mathbf{h}_{eff} due to various magnetic anisotropic contributions and due to external field acting on the free layer can be written as,

$$\mathbf{h}_{\text{eff}} = (h_a + h_b)m^x \mathbf{e}^x + h_e \mathbf{e}^y - N_z m^z \mathbf{e}^z. \quad (2)$$

Magnetization of the free layer taken for our study is aligned along its easy axis (x -axis) and hence magneto-crystalline anisotropy acts along x -axis. h_a is the field term due to magneto-crystalline anisotropy and \mathbf{e}^x is the unit vector along x -axis. h_b is biquadratic coupling field arises due to the uncompensated magnetic poles present in the edges of the both pinned layers and its value can be written as^{19,46},

$$h_b = \frac{\mu_0 M_s^2 \delta^2 L}{2\pi^3 A_{ex} d} \exp\left(\frac{-4\pi t_s}{L}\right) \left[1 - \exp\left(\frac{-8\pi d}{L}\right)\right]. \quad (3)$$

Here, A_{ex} is the exchange stiffness constant of the free layer and t_s is the thickness of the spacer layer, δ and L are height and period of the roughness of the pinned layer respectively. In Eq. (2), h_e represents the external magnetic field applied perpendicular to the easy axis of the magnetization (along y -direction) and \mathbf{e}^y is the unit vector along y -axis. N_z represents the demagnetization factor along z -direction, which arises due to the shape anisotropy present in the system and \mathbf{e}^z is the unit vector along z -axis. For our case, $\theta_1 = \theta_2 = 0$ and hence $\mathbf{m}_{p1} = \mathbf{e}^x$, $\mathbf{m}_{p2} = -\mathbf{e}^x$. By substituting these values and the total effective magnetic field found in Eq. (2) into Eq. (1), and write the LLGS equation in component form as,

$$\begin{aligned} \frac{dm^x}{d\tau} = & (h_e + N_z m^y) m^z - \alpha [h_e m^x m^y \\ & - (h_a + h_b + N_z) m^x m^{z^2} - (h_a + h_b) m_x m_y^2] \\ & - a_{j1} (m^{y^2} + m^{z^2}) - a_{j2} (m^{y^2} + m^{z^2}) \end{aligned} \quad (4a)$$

$$\begin{aligned} \frac{dm^y}{d\tau} = & -(h_a + h_b + N_z) m^x m^z \\ & + \alpha [(h_e - (h_a + h_b) m^y) m^{x^2} + (h_e + N_z m^y) m^{z^2}] \\ & + a_{j1} m^x m^y + a_{j2} m^x m^y \end{aligned} \quad (4b)$$

$$\begin{aligned} \frac{dm^z}{d\tau} = & (h_a + h_b) m^x m^y - h_e m^x - \alpha [(h_a + h_b + N_z) m^{x^2} m^z \\ & + (h_e + N_z m^y) m^y m^z] + a_{j1} m^x m^z + a_{j2} m^x m^z. \end{aligned} \quad (4c)$$

Eqs. (4a - 4c) are the first order dimensionless LLGS equations by solving the set of above three equations, magnetization switching dynamics of the free layer can be studied and it is discussed in the next section.

III. MAGNETIZATION SWITCHING DYNAMICS: A NUMERICAL STUDY

The set of three first order dimensionless LLGS equations (Eqs. (4a - 4c)) are numerically integrated using Runge-Kutta fourth order procedure and the material parameters used for the numerical simulation are given in TABLE I. After solving the dimensionless LLGS equations, the dimensionless time variable τ is converted into dimension time variable t by using the transformation

$t = \tau / \gamma M_s$. In order to suppress the ringing effect and oscillations in the magnetization switching, we have chosen the value of applied current density and Gilbert damping factor as, $J = 10 \times 10^{11} \text{ Am}^{-2}$ and $\alpha = 0.001$ respectively. First, the impact of biquadratic coupling on switching time is studied, by separately solving the LLGS equation for both in the absence of biquadratic coupling and in the presence of biquadratic coupling case. Then impact of period of roughness and spacer layer thickness on switching time are studied by varying their respective parameter. Numerical results of each study is presented in the forthcoming sections.

Parameter	Symbol	Value
Polarization factor	p	0.3
Gilbert damping parameter	α	0.001
Magneto-crystalline anisotropy field of the free layer	h_a	0.01
Saturation magnetization of the free layer	M_s	$0.795 \times 10^6 \text{ Am}^{-1}$
Thickness of the free layer	d	$2.8 \times 10^{-9} \text{ m}$
Thickness of spacer layer	t_s	$2 \times 10^{-9} \text{ m}$
Exchange stiffness constant of the free layer	A_{ex}	$2.1 \times 10^{-11} \text{ Jm}^{-1}$
Height of the roughness of the pinned layer	δ	$0.8 \times 10^{-9} \text{ m}$
Period of the roughness of the pinned layer	L	$40 \times 10^{-9} \text{ m}$

TABLE I. Values of various parameters used for the calculations^{21,22}.

A. Impact of biquadratic coupling on switching time

First, the set of three first order LLGS equations (Eqs. (4a - 4c)) are numerically simulated in the absence of biquadratic coupling and in the presence of biquadratic coupling case separately and the results obtained are plotted in FIGURE 2. The magnetization (\mathbf{m}) of the free layer is initially aligned along the positive x -direction ($m^x = +1$). The current passes through the pinned layer becomes spin polarized and the polarized electrons entered into free layer produces a spin transfer torque. As a response to the spin transfer torque and damping torque, the free layer magnetization undergoes an elliptical precession and reaches the switched state ($m^x = -1$). The time taken for switch the magnetization from $m^x = +1$ to $m^x = -1$ is called as switching time and its value in the absence of biquadratic coupling is 186 ps for an applied current density of $10 \times 10^{11} \text{ Am}^{-2}$. The presence of biquadratic coupling reduces the switching time to 160 ps (shown in FIGURE 2). The reason for reduction of switching time in the presence of biquadratic coupling is understood from the magnetization trajectory in $m^y - m^z$ plane shown in the FIGURE 3. In the absence of biquadratic coupling, the free layer magnetization reaches the hard axis $m^y = +1$ near $m^z = -0.45$ as a response

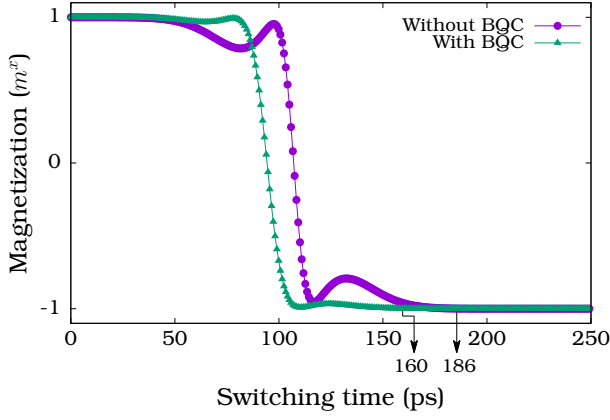


FIG. 2. A plot of free layer magnetization versus switching time for the pentalayer nanopillar in the presence and in the absence of the biquadratic coupling for an applied current density of $J = 10 \times 10^{11} \text{ Am}^{-2}$. The presence of biquadratic coupling reduces the switching time from 186 ps to 160 ps.

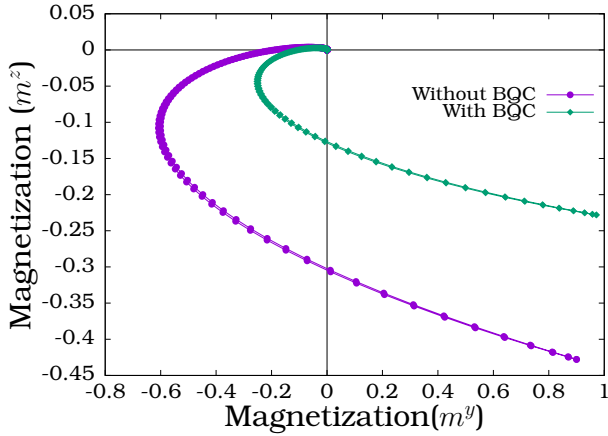


FIG. 3. Magnetization trajectory in $m^y - m^z$ plane for the presence of biquadratic coupling and for the absence of biquadratic coupling (BQC).

to spin transfer torque, whereas in the presence of biquadratic coupling, the free layer magnetization reaches the hard axis $m^y = +1$ near $m^z = -0.20$ itself. i.e. The spiralling path of the free layer magnetization in $m^y - m^z$ plane in the presence of biquadratic coupling is very short compared to that of the same in the absence of biquadratic coupling. Additional biquadratic coupling field arises due to the uncompensated magnetic poles presented in the edges of the pinned layers, moves the magnetization of the free layer from easy axis to hard axis very fast and hence the presence of biquadratic coupling reduces the switching time. Therefore, the fastest magnetization switching in pentalayer structure can be achieved in the presence of biquadratic coupling and it is in good agreement with the results obtained for the trilayer structure²². Since, biquadratic coupling arises due

to the roughness in the pinned layer, we study the impact of period of roughness on switching time and the results of the same are presented in the next section.

B. Impact of Period of Roughness on Switching Time

In order to understand the effect of period of roughness on switching time, the first order LLGS equations (Eqs. (4a - 4c)) are numerically integrated by varying the period of the roughness (L) from 0 nm to 100 nm. The data obtained from numerical simulations for an applied current density of $10 \times 10^{11} \text{ Am}^{-2}$ are plotted in FIGURE 4. Switching time in the absence of biquadratic coupling

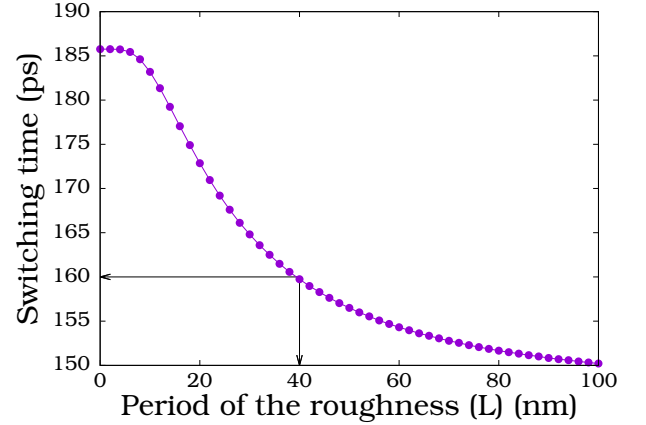


FIG. 4. A plot of the period of the roughness versus switching time for the pentalayer nanopillar for an applied current density $J = 10 \times 10^{11} \text{ Am}^{-2}$. Switching time decreases when the period of the roughness is decreased.

(i.e. if there is no roughness) is 186 ps and when the period of roughness is increased, switching time of the free layer magnetization decreases, and it saturates near 100 nm. When the period of roughness increases, the uncompensated magnetic poles presented in the edges of the pinned layers are increased and it increases the biquadratic coupling field acting on the free layer which reduces the switching time. For the period of roughness of our device (40 nm), switching time is 160 ps, which is perfectly matches with the result in FIGURE 2. Impact of spacer layer thickness on switching time is also studied and their numerical results are presented in the next section.

C. Impact of Spacer Layer Thickness on Switching Time

Effect of spacer layer thickness on switching time is studied by numerically simulating the first order LLGS equations given in Eqs. (4a - 4c), by varying the spacer layer thickness from 1 nm to 10 nm. The data obtained for the applied current density of $10 \times 10^{11} \text{ Am}^{-2}$ are

plotted in FIGURE 5. Switching time increases from

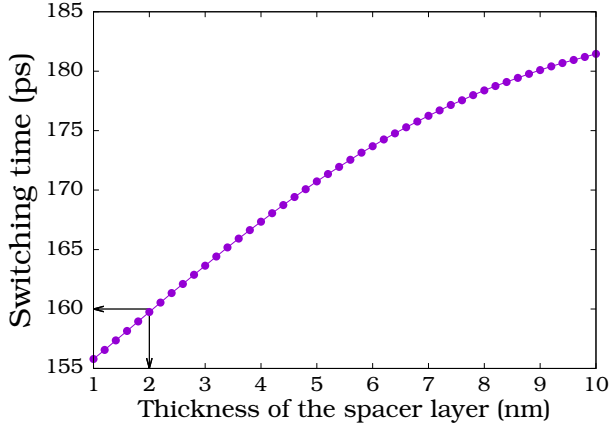


FIG. 5. A plot of the thickness of the spacer layer versus switching time for the pentalayer nanopillar for an applied current density $J = 10 \times 10^{11} \text{ Am}^{-2}$. Switching time increases when the thickness of the spacer layer is increased.

155 ps to 182 ps, when the thickness of the spacer layer is increased from 1 nm to 10 nm (shown in FIGURE 5). Biquadratic coupling field acting on the free layer decreases exponentially, when the thickness of the spacer layer is increased, and hence the switching time increases. After 10 nm, the effect due to biquadratic coupling is negligible and switching occurs only due to spin transfer torque. For the thickness of the spacer layer of our device (2 nm), switching time is 160 ps, and it exactly matches with the result in FIGURE 2.

IV. CONCLUSION

The spin transfer torque assisted magnetization switching in the pentalayer nanopillar with biquadratic coupling is studied by numerically solving the LLGS equation. The presence of biquadratic coupling reduces the switching time from 186 ps to 160 ps for an applied current density of $10 \times 10^{11} \text{ Am}^{-2}$. Reduction of switching time in the presence of biquadratic coupling is also confirmed by the magnetization trajectory in m^y - m^z plane. Further, the effect of period of roughness and spacer layer thickness on switching time is also studied. Switching time of the free layer in the pentalayer nanopillar device can be reduced by fabricating the pentalayer nanopillar with biquadratic coupling and with minimal thickness.

ACKNOWLEDGMENTS

D. A acknowledges Department of Science and Technology (DST) for the award of DST-INSPIRE Fellowship. P. S acknowledges DST for the award of SERB - Young Scientist project (SB/FTP/PS-061/2013).

- ¹C. Chappert, A. Fert, and F. N. Van Dau, *Nat. Mater.* **6**, 813 (2007).
- ²J. A. Katine and E. E. Fullerton, *J. Magn. Magn. Mater.* **320**, 1217 (2008).
- ³S. Kaka, M. R. Pufall, W. H. Rippard, T. J. Silva, S. E. Russek, and J. A. Katine, *Nature* **437**, 389 (2005).
- ⁴M. Carpentieri and F. Lattarulo, *IEEE Trans. Magn.* **49**, 3151 (2013).
- ⁵J. C. Slonczewski, *J. Magn. Magn. Mater.* **159**, L1 (1996).
- ⁶Z. Li and S. Zhang, *Phys. Rev. B* **68**, 024404 (2003).
- ⁷G. D. Fuchs, I. N. Krivorotov, P. M. Braganca, N. C. Emley, A. G. F. Garcia, D. C. Ralph, and R. A. Buhrman, *Appl. Phys. Lett.* **86**, 152509 (2005).
- ⁸L. Berger, *J. Appl. Phys.* **93**, 7693 (2003).
- ⁹H. Meng, J. Wang, and J.-P. Wang, *Appl. Phys. Lett.* **88**, 082504 (2006).
- ¹⁰Y. Huai, M. Pakala, Z. Diao, and Y. Ding, *Appl. Phys. Lett.* **87**, 222510 (2005).
- ¹¹R.-X. Wang, P.-B. He, Z.-D. Li, A.-L. Pan, and Q.-H. Liu, *J. Appl. Phys.* **109**, 033905 (2011).
- ¹²D. Apalkov, M. Pakala, and Y. Huai, *J. Appl. Phys.* **99**, 08B907 (2006).
- ¹³G. Finocchio, B. Azzerboni, G. D. Fuchs, R. A. Buhrman, and L. Torres, *J. Appl. Phys.* **101**, 063914 (2007).
- ¹⁴N. N. Mojmader, C. Augustine, D. E. Nikonov, and K. Roy, *J. Appl. Phys.* **108**, 104306 (2010).
- ¹⁵A. Makarov, V. Sverdlov, D. Osintsev, and S. Selberherr, *Phys. Status Solidi RRL* **5**, 420 (2011).
- ¹⁶Z. Diao, A. Panchula, Y. Ding, M. Pakala, S. Wang, Z. Li, D. Apalkov, H. Nagai, A. Driskill-Smith, L.-C. Wang, E. Chen, and Y. Huai, *Appl. Phys. Lett.* **90**, 132508 (2007).
- ¹⁷B. S. Chun, C. Fowley, M. Abid, and J. M. D. Coey, *J. Phys. D: Appl. Phys.* **43**, 025002 (2010).
- ¹⁸M. D. Stiles, in *Ultrathin Magnetic Structures III*, edited by J. Bland and B. Heinrich (Springer Berlin Heidelberg, 2005) pp. 99–142.
- ¹⁹S. Demokritov, E. Tsybmal, P. Grünberg, W. Zinn, and I. K. Schuller, *Phys. Rev. B* **49**, 720 (1994).
- ²⁰L. Néel, *C. R. Acad. Sci.*, **255**, 1676 (1962).
- ²¹D. Aravinthan, P. Sabareesan, and M. Daniel, *AIP Advances* **5**, 077166 (2015).
- ²²D. Aravinthan, P. Sabareesan, and M. Daniel, *AIP Conf. Proc.* **1731**, 130032 (2016).
- ²³M. Rührig, R. Schfer, A. Hubert, R. Mosler, J. A. Wolf, S. Demokritov, and P. Grünberg, *Phys Status Solidi (a)* **125**, 635 (1991).
- ²⁴S. O. Demokritov, *J. Phys. D: Appl. Phys.* **31**, 925 (1998).
- ²⁵P. Grünberg, S. Demokritov, A. Fuss, M. Vohl, and J. A. Wolf, *J. Appl. Phys.* **69**, 4789 (1991).
- ²⁶J. Unguris, R. J. Celotta, and D. T. Pierce, *Phys. Rev. Lett.* **67**, 140 (1991).
- ²⁷D. T. Pierce, J. Unguris, and R. J. Celotta, in *Ultrathin Magnetic Structures II*, edited by J. A. C. Bland and B. Heinrich (Springer Berlin Heidelberg, 2005) pp. 117–147.
- ²⁸E. E. Fullerton, K. T. Riggs, C. H. Sowers, S. D. Bader, and A. Berger, *Phys. Rev. Lett.* **75**, 330 (1995).
- ²⁹H. J. Elmers, G. Liu, H. Fritzsche, and U. Gradmann, *Phys. Rev. B* **52**, R696 (1995).
- ³⁰J. Meersschaut, J. Dekoster, R. Schad, P. Beliën, and M. Rots, *Phys. Rev. Lett.* **75**, 1638 (1995).
- ³¹A. Schreyer, J. F. Ankner, T. Zeidler, H. Zabel, C. F. Majkrzak, M. Schäfer, and P. Grünberg, *Europhys. Lett.* **32**, 595 (1995).
- ³²M. Grimsditch, S. Kumar, and E. E. Fullerton, *Phys. Rev. B* **54**, 3385 (1996).
- ³³R. Hicken, C. Daboo, M. Gester, A. Ives, S. Gray, and J. A. C. Bland, *Thin Solid Films* **275**, 199 (1996).
- ³⁴A. Azevedo, C. Chesman, S. M. Rezende, F. M. de Aguiar, X. Bian, and S. S. P. Parkin, *Phys. Rev. Lett.* **76**, 4837 (1996).
- ³⁵R. P. Erickson, K. B. Hathaway, and J. R. Cullen, *Phys. Rev. B* **47**, 2626 (1993).

- ³⁶D. Edwards, J. Ward, and J. Mathon, J. Magn. Magn. Mater. **126**, 380 (1993).
- ³⁷J. Barnaš and P. Grünberg, J. Magn. Magn. Mater. **121**, 326 (1993).
- ³⁸J. Inoue, J. Magn. Magn. Mater. **136**, 233 (1994).
- ³⁹D. Spišák and J. Hafner, J. Magn. Magn. Mater. **168**, 257 (1997).
- ⁴⁰J. C. Slonczewski, Phys. Rev. Lett. **67**, 3172 (1991).
- ⁴¹J. Slonczewski, J. Magn. Magn. Mater. **150**, 13 (1995).
- ⁴²J. C. Slonczewski, J. Appl. Phys. **73**, 5957 (1993).
- ⁴³U. Rücker, S. Demokritov, E. Tsymbal, P. Grnberg, and W. Zinn, J. Appl. Phys. **78**, 387 (1995).
- ⁴⁴D. Aravinthan, P. Sabareesan, and M. Daniel, J. Magn. Magn. Mater. **421**, 409 (2017).
- ⁴⁵M. Daniel and P. Sabareesan, J. Magn. Magn. Mater. **322**, 675 (2010).
- ⁴⁶T. G. S. M. Rijks, R. F. O. Reneerkens, R. Coehoorn, J. C. S. Kools, M. F. Gillies, J. N. Chapman, and W. J. M. de Jonge, J. Appl. Phys. **82**, 3442 (1997).